Scientific
Research
Publishing

Investigation of Non-Thermodynamical CO₂ Adsorption Behavior for Amine-Modified Nanoporous Silica

Kazuhisa Yano*, Norihiko Setoyama, Kenzo Fukumori

Toyota Central R & D Labs Inc., 41-1 Yokomichi, Nagakute, Aichi, Japan
Email: *k-yano@mosk.tytlabs.co.jp

Abstract

Non-thermodynamical CO_2 adsorption behavior for amine-modified nanoporous silica is clarified by evaluating the mobility of organic functional group inside mesopores by using pulsed NMR technique. CO_2 adsorption behavior of nanoporous silica modified with amino-propyl silane (AP) changes significantly depending on the amount of AP loaded. A low AP loaded sample shows normal adsorption behavior; the amount of CO_2 adsorbed decreases with increasing temperature. In contrast, a high AP loaded sample possesses non-thermodynamic CO_2 adsorption behavior in which the amount of CO_2 adsorbed increases with increasing temperature in within a certain temperature range. To address the mechanism, a pulsed NMR technique was employed to clarify the mobility of AP molecules, and it was found that the mobility of mobile components in a high AP loaded sample increased drastically with increasing temperature while the mobility in a low AP loaded sample remained unchanged. It is understood that the enhancement of the diffusion of CO_2 inside nanopores leads to the non-thermodynamic adsorption behavior.

1. Introduction

Global warming caused by the increase of the amount of CO_2 emission is a serious problem to be solved immediately. The methods using CO_2 absorbing solution are useful and already commercialized in some coal-fired power plants or

factories. However, in the method, heating of absorbing solution, usually water, is required to recover CO_2 from the solution, which consumes a lot of energy. To decrease energy requirements in a CO_2 separation system, the development of high performance CO_2 adsorbent is desired [1] [2].

Various types of porous materials such as zeolite [3] [4] [5] [6] [7], porous carbons [8] [9] [10] [11] [12], MOFs [13] [14] [15] [16] [17], have been investigated as an adsorbent for CO_2. We have been conducted the synthesis and applications of mesoporous silica spheres that have uniform particle size and pore structure [18] [19] [20]. Amino-moieties were incorporated into mesoporous silica by a co-condensation method and its catalytic performance was optimized by changing particle size or pore diameter [21] [22] [23]. Amino-group incorporated mesoporous silica is considered to be a good candidate for a CO_2 adsorbent, and is investigated by many researchers [24] [25].

Emission gases of factories or power supply facilities contain a lot of water vapor. If the selectivity for water vapor is higher than that for CO_2, it is required to remove water vapor from the emission. This process consumes a lot of energy, and developing the adsorbent with higher CO_2 selectivity is crucial.

Generally, adsorption of a gas follows Clausius-Clapeyron equation. At higher temperature, an adsorption isotherm shifts to the higher pressure side and the amount of adsorbed gas at the same pressure decreases. The tendency is the same for water vapor, leading to the decrease of adsorbed amount at higher temperature. Opposite CO_2 adsorption behavior was observed for polyethyleneimine-impregnated materials [26] and amino-modified porous silicas [27] [28]. The amount of CO_2 adsorbed increased upon the increase of the temperature. A porous material with this non-thermodynamic adsorption behavior is expected to be a high CO_2 selection adsorbent for the emission gases of factories.

Amino-propyl (AP) modified nanoporous silicas with different AP amounts have been synthesized by a co-condensation method, and the effect of AP amount on CO_2 adsorption behavior has been evaluated. The non-thermodynamic adsorption behavior is observed for a high AP loaded material. In contrast, the amount of CO_2 adsorbed decreases with increasing temperature for a low AP loaded material. To understand this behavior difference, a pulsed NMR technique is adopted to clarify the mobility of AP molecules in AP loaded nanoporous silicas at different temperature. As a result, a distinct difference is observed in the mobility.

2. Experimental

2.1. Materials

3-Aminopropyltrimethoxysilane (AP-TMS) was purchased from Aldrich. Hexadecyltrimethylammonium chloride (C_{16}TMACl) and tetramethoxysilane (TMOS) were purchased from Tokyo Kasei (Japan). Methanol and 1N sodium hydroxide solution were purchased from Wako Pure Chemical Co (Japan). All materials were used as received.

2.2. Synthesis of Nanoporous Silica Spheres

Amino propy-modified nanoporous silica particles were obtained according to the literature [22]. In a typical synthesis, 3.52 g of C_{16}TMACl and 2.28 mL of 1 M sodium hydroxide solution were dissolved in 800 g of methanol/ water (50/50 = w/w) solution. A mixture of 1.19 g (7.81 mmol) of TMOS and 0.16 g (0.87 mmol) of AP-TMS (AP-TMS/(TMOS + AP-TMS) = 10 mol%) were then added to the solution with vigorous stirring at 298 K. After the addition of the TMOS and APTMS, the clear solution suddenly turned opaque and resulted in a white precipitate. After 8 h of continuous stirring, the mixture was aged overnight. The white powder was filtered and washed with distilled water at least three times, and then dried at 45°C for 72 h. The powder obtained was heated in a 60 ml of ethanol solution containing a 1 ml of concentrated hydrochloric acid at 333 K for 3 h to remove the surfactant. Then, the powder was filtered, washed several times with ethanol, and dried at 318 K. Then, the amino propyl modified material was treated with an ammonia solution to remove any residual Cl^- ions and to neutralize the protonated amines in the sample [22]. A 0.35 g of the modified sample was suspended in a 20 ml of methanol solution containing a 1 ml of ammonia solution (28%) at room temperature for 8 h. The solid was recovered by filtration, washed with methanol, and finally dried in a vacuum at 423 K for 12 h.

2.3. Characterization

Scanning electron micrographs (SEMs) were obtained with a SU3500 (Hitachi). Powder X-ray diffraction measurement was carried out with a Rigaku Rint-2200 X-ray diffractometer using Cu-Kα radiation. Nitrogen adsorption/ desorption isotherms were measured using a BELSORP-mini II (Bell-Japan) at 77 K. Samples were evacuated at 423 K under 0.13 Pa before the measurement. Pore volume was estimated from the amount of adsorbed nitrogen at the relative pressure of 0.95. Pore diameter was calculated by the BJH method for the adsorption branch. CO_2 adsorption isotherms were measured using a BELSORP-MAX-12-N-T-HL at different temperatures. N elemental analyses (EA) were carried out on an Elementer varioEL elemental analyzer.

2.4. Pulsed NMR Measurements

The mobility of amino moieties was evaluated by pulsed NMR measurements that measure relaxation time of ^1H which is one of the main constituent elements of amino moieties. The pulsed NMR measurements were performed with JEOL-JNM-MU25A spectrometer operating at 25 MHz for protons (^1H) in the phase-sensitive detection mode. Spin-spin relaxation time (T_2) was measured for ca. 1 g of sample in a 10 mmϕ sample tube [29]. Samples were evacuated at 423K under 0.13 Pa before the measurement to remove adsorbed water. The pulse sequences for T_2 measurements were the solid echo pulse sequences ($90°_x \tau 90°_y$: 90° pulse width = 2 μs, τ = 8 μs, pulse repetition time = 4 - 10 s, cumulated number

= 64 - 128). The measurements were conducted from 30°C to 130°C with 20°C interval. The data for the decay process of the traverse magnetization decay signal $M(t)$ is analyzed as the sum of the one Gaussian component for short T_2 and one single exponential component for long T_2 as expressed by Eq. (1):

$$M(t) = A_S \exp\left[-\left(\frac{t}{T_{2S}}\right)^2\right] + A_L \exp\left[-\frac{t}{T_{2L}}\right] \tag{1}$$

where A_S and A_L are the amplitude for the short and long component. T_{2S} and T_{2L} are the corresponding T_2 values. The fraction of short and long component, f_S and f_L are determined from A_S and A_L values.

3. Results and Discussion

3.1. Effect of Amount of AP on CO$_2$ Adsorption Behovior

Nanoporous silica samples obtained by co-condensation using 10, 30, and 50 mol % of AP-TMS are denoted as AP10, AP30, and AP50, respectively, according to the AP-TMS ratio in the synthesis. The content of nitrogen increases with increasing the ratio of AP-TMS, and results are listed in **Table 1**. Nitrogen adsorption-desorption isotherms of samples are shown in **Figure 1**. A steep increase between P/P$_0$ of 0.2 and 0.3 indicates the existence of mesopores in AP10. However, AP30 and AP50 are found to adsorb much less nitrogen than AP10. Physical properties of samples are also summarized in **Table 1**. Specific surface area, pore size and pore volume of AP10 are comparable to that in ref 20. Those values are much smaller for AP30 and AP50. Powder XRD measurements were conducted and corresponding XRD patterns are shown in **Figure 2**. A sharp peak around 2° ascribed to d$_{100}$ periodicity of mesopores is observed for AP10. The pattern is typical of mesoporous silica. No peak is observed for AP30 and AP50. This indicates that no regular pore structure exists in AP30 and AP50.

Table 1. Properties of samples.

Sample Name	N content [mmol/g]	Specific surface area [m²/g]	Pore diameter [nm]	Pore volume [ml/g]
AP10	0.7	850	2.2	0.34
AP30	3.0	8.1	-	0.01
AP50	3.9	10.2	-	0.02
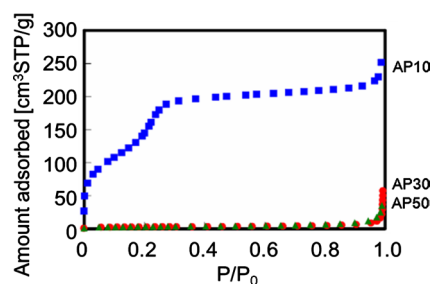
Figure 1. Nitrogen adsorption isotherms of AP10, AP30 and AP50.

Figure 3 shows SEM images of samples. All particles are in sub-micron range between 0.41 μm and 0.68 μm.

CO_2 adsorption isotherms of samples at different temperatures are shown in Figure 4. As for AP10, adsorbed amount of CO_2 decreases with increasing
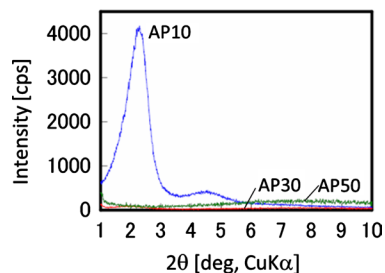
Figure 2. XRD patterns of AP10, AP30 and AP50.
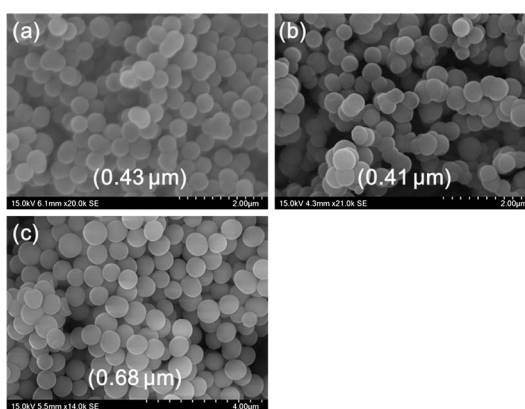
Figure 3. SEM images of (a) AP10, (b) AP30 and (c) AP50. Average particle diameters are in parentheses.
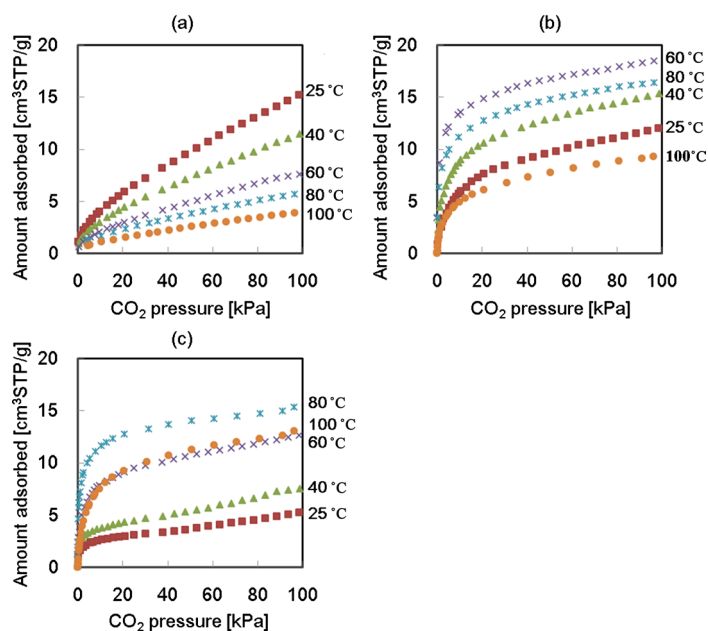
Figure 4. CO_2 adsorption isotherms of samples at different temperatures: (a) AP10, (b) AP30, (c) AP50.

temperature. This tendency is quite normal. In contrast, the amount of CO_2 adsorbed increases with increasing temperature for AP30 and AP50 in some temperature range. The amount is the largest at 60°C and decreases at higher temperature for AP30. This behavior is non-thermodynamic and does not follow the Clausius-Clapeyron equation. As for AP30, the pores are mostly fulfilled with amino moieties, and a few spaces exist at lower temperature. In this case, only a limited amount of CO_2 is captured. However, once amino moieties are more mobile and active at higher temperature, CO_2 molecules could easily penetrate into inside pores to be captured. The optimum temperature for AP50 is 80°C which is higher than the temperature for AP30. Since much more amount of AP molecules are contained in pores of AP50, higher temperature would be needed for amino-moieties to be mobile.

It is found that CO_2 adsorption behavior changes drastically by adjusting the amount of amino moieties in nanoporous silica. AP10 adsorbs more CO_2 at lower temperature while AP30 and AP50 adsorb more CO_2 at higher temperature. It is interesting that the CO_2 adsorption behavior is highly affected by the ratio of AP loaded.

3.2. Mobility of Amino Moieties

It is mentioned that amino-moieties of AP30 or AP50 are more mobile at higher temperature. To investigate the effect of temperature on the mobility of amino moieties in samples, the pulsed NMR measurements were conducted for AP10 and AP30 that show different temperature dependence in CO_2 adsorption. Normalized T_2 decay curves at different temperatures are shown in Figure 5. A curve is deconvoluted to a short and long component according to Equation (1). Table 2 summarizes spin-spin relaxation time for short (T_{2S}) and long (T_{2L}) component and corresponding fractions (f_S, f_L) for AP10 and AP30. A short relaxation time means that molecules are rigid, and long relaxation time reveals molecules are more mobile.

As for AP10, T_{2S} and T_{2L} are almost the same value against temperature, indicating that the mobility of the AP molecules unchanged. However, the fraction of rigid component, f_S, decreases and the more mobile component, f_L, increases with increasing temperature. The behavior can easily be understood by plotting the data (Figure 6). F_S is 52% at 30°C and the value decreases to 38% at 130°C.

The exact opposite tendency is observed for AP30. F_S and f_L remain unchanged against temperature, and T_{2L} increases drastically with increasing temperature. The f_S:f_L ratio is almost 74:26 and the ratio remains unchanged upon temperature increase. The f_S of AP30 is much larger than that of AP10, implying that the amount of rigid AP molecules is much larger for AP30. T_{2S} slightly increases from 11 μs to 16 μs whereas T_{2L} increases from 32 μs to 97 μs. The increase of the relaxation time for the mobile component is significant. T_{2S} for the rigid component of AP30 is much smaller than that of AP10, suggesting that many of AP molecules in AP30 are confined more tightly. This could be caused
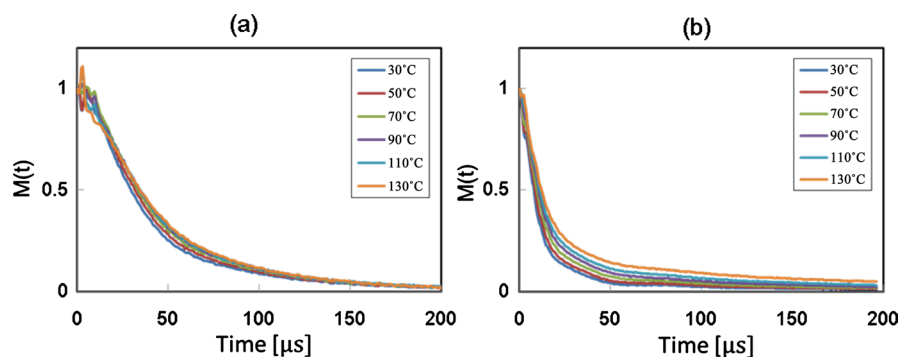
Figure 5. Normalized T2 decay carves for (a) AP10 and (b) AP30 at different temperatures.

Table 2. Summary of spin-spin relaxation time and corresponding fractions.

Temperature (°C)	AP10		AP30	
	T_{2S} (µs) [f_S (%)]	T_{2L} (µs) [f_L (%)]	T_{2S} (µs) [f_S (%)]	T_{2L} (µs) [f_L (%)]
30	34 [52%]	59 [48%]	11 [72%]	32 [28%]
50	36 [53%]	63 [47%]	12 [74%]	41 [26%]
70	38 [53%]	65 [47%]	13 [75%]	53 [25%]
90	39 [47%]	63 [53%]	14 [75%]	63 [25%]
110	40 [43%]	61 [57%]	15 [74%]	75 [26%]
130	40 [38%]	60 [62%]	16 [73%]	97 [27%]
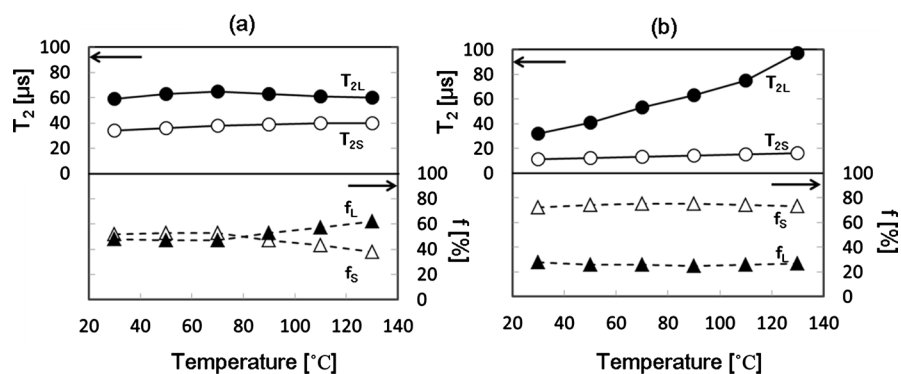
Figure 6. Temperature dependence of T_2 and fraction for (a) AP10 and (b) AP30.

by the incorporation of larger amount of AP molecules into nanopores. Conversely, T_{2L} of AP30 at higher temperature is bigger than that of AP10 although the values are lower at temperatures lower than 90°C. Therefore, the increase of the amount of CO_2 adsorbed at higher temperature could be related to the increase of the mobility of AP molecules. Although the optimum temperature for

CO_2 adsorption is different from the result obtained in the NMR experiments, the difference could be caused by the difference in atmosphere, with or without CO_2, or the length of time for the measurement.

Since the fraction and mobility of soft components in AP10 changed little, the diffusion of CO_2 was not affected by the temperature. As a result, CO_2 adsorption occurred thermodynamically. In contrast, the mobility of soft components in AP30 increased drastically with increasing temperature, leading to non-thermodynamic adsorption behovior.

4. Conclusion

By increasing the amount of amino propyl moieties (AP) incorporated into nanoporous silica, CO_2 adsorption behovior changes drastically. A low AP loaded sample adsorbs more CO_2 at lower temperature while higher AP loaded samples adsorb more CO_2 at higher temperature. To understand the mechanism, a pulsed NMR technique was employed. It was found that the mobility of mobile component in a high AP loaded sample increased drastically with increasing temperature while the mobility in a low AP loaded sample remained unchanged. The increase in the mobility in the high AP loaded sample could enhance the diffusion of CO_2 inside nanopores leading to the non-thermodynamic adsorption behovior.

Conflicts of Interest

The authors declare no conflicts of interest regarding the publication of this paper.

References

[1] Fayaz, M. and Sayari, A. (2017) Long-Term Effect of Steam Exposure on CO_2 Capture Performance of Amine-Grafted Silica. *ACS Applied Materials & Interfaces*, **9**, 43747-43754. https://doi.org/10.1021/acsami.7b15463

[2] Zhang, Z., Ma, X., Wang, D., Song, C. and Wang, Y. (2012) Development of Silica-Gel-Supported Polyethylenimine Sorbents for CO_2 Capture from Flue Gas. *AIChE Journal*, **58**, 2495-2502. https://doi.org/10.1002/aic.12771

[3] Banerjee, R., Phan, A., Wang, B., Knobler, C., Furukawa, H., O'Keeffe, M. and Yaghi, O.M. (2008) High-Throughput Synthesis of Zeolitic Imidazolate Frameworks and Application to CO_2 Capture. *Science*, **319**, 939-943. https://doi.org/10.1126/science.1152516

[4] Chen, C., Park, D.-W. and Ahn, W.-S. (2014) CO_2 Capture Using Zeolite 13X Prepared from Bentonite. *Applied Surface Science*, **292**, 63-67. https://doi.org/10.1016/j.apsusc.2013.11.064

[5] Garshasbi, V., Jahangiri, M. and Anbia, M. (2017) Equilibrium CO_2 Adsorption on Zeolite 13X Prepared from Natural Clays. *Applied Surface Science*, **393**, 225-233. https://doi.org/10.1016/j.apsusc.2016.09.161

[6] Phan, A., Doonan, C.J., Uribe-Romo, F.J., Knobler, C.B., O'Keeffe, M. and Yaghi, O.M. (2010) Synthesis, Structure, and Carbon Dioxide Capture Properties of Zeolitic Imidazolate Frameworks. *Accounts of Chemical Research*, **43**, 58-67.

https://doi.org/10.1021/ar900116g

[7] Su, F.S., Lu, C.Y., Kuo, S.C. and Zeng, W.T. (2010) Adsorption of CO_2 on Amine-Functionalized Y-Type Zeolites. *Energy Fuels*, **24**, 1441-1448. https://doi.org/10.1021/ef901077k

[8] Shafeeyan, M.S., Daud, W.M.A.W., Houshmand, A. and Shamiri, A. (2010) A Review on Surface Modification of Activated Carbon for Carbon Dioxide Adsorption. *Journal of Analytical and Applied Pyrolysis*, **89**, 143-151. https://doi.org/10.1016/j.jaap.2010.07.006

[9] Xing, W., Liu, C., Zhou, Z., Zhang, L., Zhou, J., Zhuo, S., Yan, Z., Gao, H., Wang, G. and Qiao, S. (2012) Superior CO_2 Uptake of N-Doped Activated Carbon through Hydrogen-Bonding Interaction. *Energy & Environmental Science*, **5**, 7323-7327. https://doi.org/10.1039/c2ee21653a

[10] Wickramaratne, N.P. and Jaroniec, M. (2013) Importance of Small Micropores in CO_2 Capture by Phenolic Resin-Based Activated Carbon Spheres. *Journal of Materials Chemistry A*, **1**, 112-116. https://doi.org/10.1039/C2TA00388K

[11] Wickramaratne, N.P. and Jaroniec, M. (2013) Activated Carbon Spheres for CO_2 Adsorption. *ACS Applied Materials & Interfaces*, **5**, 1849-1855. https://doi.org/10.1021/am400112m

[12] Plaza, M.G., Garcia, S., Rubiera, F., Pis, J.J. and Pevida, C. (2010) Post-Combustion CO_2 Capture with a Commercial Activated Carbon: Comparison of Different Regeneration Strategies. *Chemical Engineering Journal*, **163**, 41-47. https://doi.org/10.1016/j.cej.2010.07.030

[13] Yang, D., Cho, H., Kim, J., Yang, S. and Ahn, W. (2012) CO_2 Capture and Conversion Using Mg-MOF-74 Prepared by a Sonochemical Method. *Energy & Environmental Science*, **5**, 6465-6473. https://doi.org/10.1039/C1EE02234B

[14] Choi, S., Watanabe, T., Bae, T., Sholl, D.S. and Jones, C.W. (2012) Modification of the Mg/DOBDC MOF with Amines to Enhance CO_2 Adsorption from Ultradilute Gases. *The Journal of Physical Chemistry Letters*, **3**, 1136-1141. https://doi.org/10.1021/jz300328j

[15] Aguado, S., Nicolas, C.H., Moizan-Basle, V., Nieto, C., Amrouche, H., Bats, N., Audebrand, N. and Farrusseng, D. (2011) Facile Synthesis of an Ultramicroporous MOF Tubular Membrane with Selectivity towards CO_2. *New Journal of Chemistry*, **35**, 41-44. https://doi.org/10.1039/C0NJ00667J

[16] Lu, C., Liu, J., Xiao, K. and Harris, A.T. (2010) Microwave Enhanced Synthesis of MOF-5 and Its CO_2 Capture Ability at Moderate Temperatures across Multiple Capture and Release Cycles. *Chemical Engineering Journal*, **156**, 465-470. https://doi.org/10.1016/j.cej.2009.10.067

[17] Zhao, Y., Seredych, M., Zhong, Q. and Bandosz, T.J. (2013) Superior Performance of Copper Based MOF and Aminated Graphite Oxide Composites as CO_2 Adsorbents at Room Temperature. *ACS Applied Materials & Interfaces*, **5**, 4951-4959. https://doi.org/10.1021/am4006989

[18] Yano, K. and Fukushima, Y. (2004) Synthesis of Mono-Dispersed Mesoporous Silica Spheres with Highly Ordered Hexagonal Regularity using Conventional Alkyltrimethylammonium Halide as a Surfactant. *Journal of Materials Chemistry*, **14**, 1579-1584. https://doi.org/10.1039/b313712k

[19] Nakamura, T., Mizutani, M., Nozaki, H., Suzuki, N. and Yano, K. (2007) Formation Mechanism for Monodispersed Mesoporous Silica Spheres and Its Application to the Synthesis of Core/Shell Particles. *The Journal of Physical Chemistry C*, **111**, 1093-1100. https://doi.org/10.1021/jp0648240

[20] Yano, K. and Nishi, T. (2013) A Novel Route to Highly Monodispersed Mesoporous Silica Spheres Consisting of Nano-Sized Particles. *Microporous and Mesoporous Materials*, **158**, 257-263. https://doi.org/10.1016/j.micromeso.2012.03.043

[21] Suzuki, T.M., Yamamoto, M., Fukumoto, K., Akimoto, Y. and Yano, K. (2007) Investigation of Pore Size Effects on Base Catalysis Using Amino-Functionalized Monodispersed Mesoporous Silica Spheres as a Model Catalyst. *Journal of Catalysis*, **251**, 249-257. https://doi.org/10.1016/j.jcat.2007.08.010

[22] Suzuki, T.M., Nakamura, T., Fukumoto, K., Yamamoto, M., Akimoto, Y. and Yano, K. (2008) Direct Synthesis of Amino-Functionalized Monodispersed Mesoporous Silica Spheres and Their Catalytic Activity for Nitroaldol Condensation. *Journal of Molecular Catalysis A, Chemical*, **280**, 224-232. https://doi.org/10.1016/j.molcata.2007.11.012

[23] Suzuki, T.M., Nakamura, T., Sudo, E., Akimoto, Y. and Yano, K. (2008) Enhancement of Catalytic Performance by Creating Shell Layers on Sulfonic Acid-Functionalized Monodispersed Mesoporous Silica Spheres. *Journal of Catalysis*, **258**, 265-272. https://doi.org/10.1016/j.jcat.2008.06.021

[24] Hiyoshi, N., Yogo, K. and Yashima, T. (2005) Adsorption Characteristics of Carbon Dioxide on Organically Functionalized SBA-15. *Microporous and Mesoporous Materials*, **84**, 357-365. https://doi.org/10.1016/j.micromeso.2005.06.010

[25] Watabe, T., Nishizaka, Y., Kazama, S. and Yogo, K. (2013) Development of Amine-Modified Solid Sorbents for Postcombustion CO_2 Capture. *Energy Procedia*, **37**, 199-204. https://doi.org/10.1016/j.egypro.2013.05.102

[26] Xu, X., Song, C., Andrésen, J.M., Miller, B.G. and Scaroni, A.W. (2003) Preparation and Characterization of Novel CO_2 "Molecular Basket" Adsorbents Based on Polymer-Modified Mesoporous Molecular Sieve MCM-41. *Microporous and Mesoporous Materials*, **62**, 29-45. https://doi.org/10.1016/S1387-1811(03)00388-3

[27] Kim, S., Ida, J., Guliants, V.V. and Lin, Y. S.J. (2005) Tailoring Pore Properties of MCM-48 Silica for Selective Adsorption of CO_2. *The Journal of Physical Chemistry B*, **109**, 6287-6293. https://doi.org/10.1021/jp045634x

[28] Nik, O.G., Nohair, B. and Kaliaguine, S. (2011) Aminosilanes Grafting on FAU/EMT Zeolite: Effect on CO_2 Adsorptive Properties. *Microporous and Mesoporous Materials*, **143**, 221-229. https://doi.org/10.1016/j.micromeso.2011.03.002

[29] Fukumori, K., Kurauchi, T. and Kamigaito, O. (1989) Pulsed NMR Study of Elastomeric Block Copolymer under Deformation. *Journal of Applied Polymer Science*, **38**, 1313-1334. https://doi.org/10.1002/app.1989.070380711